Ligand Design

DOI: 10.1002/anie.201404753

B–H, C–H, and B–C Bond Activation: The Role of Two Adjacent Agostic Interactions**

Audrey Cassen, Yann Gloaguen, Laure Vendier, Carine Duhayon, Amalia Poblador-Bahamonde, Christophe Raynaud, Eric Clot, Gilles Alcaraz, and Sylviane Sabo-Etienne**

Abstract: *Tuning the nature of the linker in a L~BHR phosphinoborane compound led to the isolation of a ruthenium complex stabilized by two adjacent, δ-C–H and ε-B_{sp2}–H, agostic interactions. Such a unique coordination mode stabilizes a 14-electron "RuH_2P_2" fragment through connected σ-bonds of different polarity, and affords selective B–H, C–H, and B–C bond activation as illustrated by reactivity studies with H_2 and boranes.*

The design of functional ligands is an important strategy to achieve specific properties for a large variety of applications, and most notably in catalysis. Polyfunctional ligands offer many advantages: 1) several anchoring points to stabilize the metal center, 2) preferred geometrical positions for improvement of selectivity, 3) potential hemilabile character and access to a vacant site for further functionalization, 4) access to a large variety of functional groups with different steric and electronic properties. For example, the use of pincer-type ligands displaying a so-called non-innocent behavior led to impressive achievements in the field of small-molecule bond activation.[1]

As part of our ongoing research program on the design and coordination of bifunctional L~BHR ligands aimed at examining the B–H activation mode at a metal center, we recently disclosed a new family of ruthenium complexes incorporating a phosphinoborane ligand, $Ph_2P\sim BH(NiPr_2)$.[2] Herein, and in the absence of any pincer-type strategy which is likely to force the coordination,[3] we report the first complex exhibiting two adjacent agostic interactions of a different nature, η^2-C–H and η^2-B–H. This unique coordination mode affords selective B–H, C–H, and B–C bond activation as demonstrated by reactivity studies.

The new phosphino(benzyl)(amino)borane **1** was prepared and added to the bis(dihydrogen) ruthenium complex **2** in toluene at room temperature (Scheme 1). After work-up

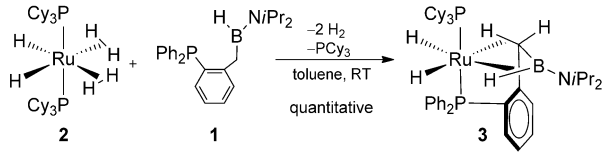

Scheme 1. Synthesis of the bis(agostic) phosphinobenzyl-(amino)borane ruthenium complex **3**.

and precipitation in cold pentane at −55 °C, a yellow powder, analyzed as $[RuH_2\{\eta^2\text{-}HB{:}\eta^2\text{-}HC\text{-}HB(NiPr_2)CH_2C_6H_4PPh_2\}(PCy_3)]$ (**3**), was isolated in 70% yield.

The complex **3** was fully characterized by NMR spectroscopy and X-ray crystallography. At room temperature, the $^{31}P\{^1H\}$ NMR spectrum of **3** displays an AB pattern at $\delta =$ 72.10 and 68.66 ppm, thus corresponding to the PCy_3 and the PPh_2 groups, respectively. The large $^2J_{PP}$ coupling constant of 241 Hz is indicative of a *trans* disposition of the two different phosphines. The $^{11}B\{^1H\}$ NMR spectrum exhibits a broad signal at $\delta = 35.5$ ppm, which is slightly more upfield than that of **1** ($\delta = 41$ ppm). The ^1H NMR spectrum at room temperature is featureless in the hydride region. At 183 K, four broad signals of equal intensity are observed at $\delta = -13.22$, −8.58, −6.71, and −1.00 ppm, in accordance with a ruthenium surrounded by four hydrogen atoms. The signal at $\delta =$ −6.71 ppm was the only one to sharpen upon boron decoupling. The four hydride signals remained broad upon phosphorus decoupling. At 213 K, the signal at $\delta = -1.00$ ppm appeared as a well-resolved doublet with a coupling constant value of 15.0 Hz, which is consistent with a $^2J_{HH}$ constant for geminal CH_2 hydrogen atoms, whereas the two hydrides at higher fields coalesced into a broad signal at approximately $\delta = -11$ ppm. (see Figures S1–S5 in the Supporting Information).[4] The broad $^{13}C\{^1H\}$ NMR resonance at $\delta =$ −11.24 ppm was assigned to the carbon atom bound to boron, thus at a much higher field than that in **1** (br, $\delta =$ 27.1 ppm). A 2D-HSQC $^{13}C/^1H\{^{31}P\}$ experiment clearly showed this strongly shielded carbon atom correlating with the two magnetically non-equivalent benzylic hydrogen atoms at $\delta = -1.00$ and 1.30 ppm, also identified by 2D-COSY $^1H\{^{31}P\}$ NMR spectroscopy (see Figures S6 and S7). To

[*] A. Cassen, Y. Gloaguen, L. Vendier, C. Duhayon, G. Alcaraz, S. Sabo-Etienne
L.C.C. (Laboratoire de Chimie de Coordination)
CNRS, Université de Toulouse, UPS, INPT
205 route de Narbonne 31077 Toulouse (France)
E-mail: gilles.alcaraz@lcc-toulouse.fr
sylviane.sabo@lcc-toulouse.fr
Homepage: http://www.lcc-toulouse.fr/lcc/spip.php?article433
A. Poblador-Bahamonde, C. Raynaud, E. Clot
Institut Charles Gerhardt, CNRS, Université de Montpellier 2
CNRS 5253, cc 1501
Place Eugène Bataillon, 34095 Montpellier (France)
C. Raynaud
Sorbonne Universités, UPMC Univ. Paris 06, CNRS UMR 7616
Laboratoire de Chimie Théorique
75005 Paris (France)

[**] We thank the CNRS and the ANR for support through the ANR program ReBAB (ANR-11-BS07-0015).

Supporting information for this article is available on the WWW under http://dx.doi.org/10.1002/anie.201404753.

provide additional support for our assignments, we synthesized the 99% ^{13}C-enriched version of **1** at the benzylic position ([^{13}C]-**1**). Its reaction with **2** led to the isolation of the corresponding ^{13}C-enriched complex [^{13}C]-**3**, thus showing, unambiguously, an intense ^{13}C NMR signal at $\delta = -12.12$ ppm (see Figure S11). A series of selective 1D-HMQC experiments recorded for [^{13}C]-**3** revealed two distinct $^{1}J_{^{13}C-H}$ coupling constant values for the benzylic CH_2 group: a large one of (138 ± 2) Hz, corresponding to an uncoordinated C–H bond ($\delta^1H = 1.36$ ppm), and a smaller one of (97 ± 2) Hz, which is indicative of a C–H δ-agostic interaction ($\delta^1H = -0.94$ ppm; see Figures S12 and S13).[5]

Crystals of **3** were grown at 235 K and the X-ray structure determined at 110 K (Figure 1 and Table 1). The Ru atom is in a distorted octahedral environment with the two phosphorus atoms in pseudoaxial positions [P1-Ru-P2: 164.91(3)°], and the equatorial plane is occupied by four coplanar hydrogen atoms (H1, H2, H3, and H11).

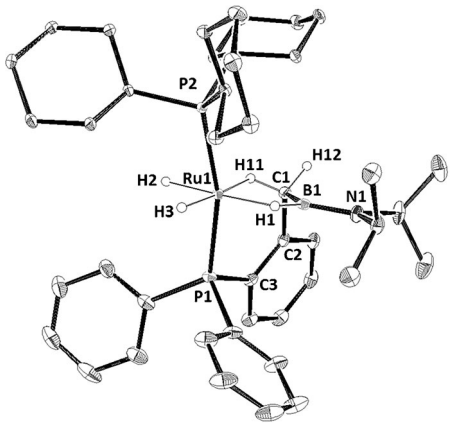

Figure 1. X-ray structure of **3**. Ellipsoids are shown at 30% probability. Hydrogen atoms of the Cy, Ph, and *i*Pr groups have been omitted for clarity.

Table 1: Selected geometrical parameters (distances in Å, angles in °) for the experimental and calculated (DFT/B3PW91) structures for **3** and **1**.

Parameter	**3**		**1**	
	Exp	Calcd	Exp	Calcd
Ru···B1	2.173(3)	2.173	–	–
Ru···C1	2.375(3)	2.376	–	–
Ru-P2	2.3298(8)	2.357	–	–
Ru-P1	2.2648(8)	2.293	–	–
Ru-H2	1.59(3)	1.611	–	–
Ru-H1	1.69(3)	1.742	–	–
Ru-H3	1.49(3)	1.583	–	–
Ru···H11	1.97(3)	1.897	–	–
Ru···H12	3.145	3.228	–	–
B1-H1	1.24(3)	1.319	1.10(2)	1.202
C1-H11	0.98(3)	1.158	0.97(3)	1.101
C1-H12	0.99(3)	1.097	1.00(3)	1.101
B1-C1	1.608(4)	1.617	1.593(3)	1.592
P1-Ru-P2	164.91(3)	163.6	–	–
B1-C1-C2	114.4(2)	115.5	113.8(2)	116.7
C1-Ru-H11	23.9(9)	28.8	–	–
C1-B1-H1	127(1)	128.8	117(1)	119.5
B1-C1-H11	114(2)	112.0	111(2)	110.1
B1-C1-H12	109(2)	111.2	107(2)	107.9

A full optimization of **3** was conducted at the DFT/B3PW91 level of theory to assess the reliability of hydrogen location by X-ray (see Computational Details in the Supporting Information). The calculated geometrical parameters for the free phosphinoborane **1** and complex **3** are in excellent agreement with the X-ray data, as can be seen in Table 1. The DFT data (see in italics below) allow us to better quantify the metrics of the agostic interactions. The Ru···H1 distance [1.69(3) Å, *1.742 Å*] and the elongated B–H1 bond [1.24(3) Å, *1.319 Å*], compared to that in **1** [1.10(2) Å, *1.202 Å*], are in the range observed for the two previously reported agostic σ-B–H Ru complexes.[2] Notably, agostic interactions resulting from the coordination of B_{sp2}–H bonds, as in true σ-borane complexes,[6] are restricted to three examples: the chromium complex [Cr{HBN($SiMe_3$)$_2$(CH=CHMe)}$(CO)_4$], described by Braunschweig et al.,[7] and the two ruthenium complexes [RuH_2{η^2-HB(N*i*Pr_2)CH_2PPh_2}-$(PCy_3)_2$] (**A**) and [RuH_2{η^2-HB(N*i*Pr_2)$C_6H_4PPh_2$}$(PCy_3)_2$] (**B**), from our group.[2] The C1-B1-H1 angle is significantly increased upon coordination [127(1)°, *128.8*° in **3** versus 117(1), *119.5*° in **1**]. The Ru···B distance [2.173(3) Å] is much shorter than that in **A** [2.7574(80) Å] or **B** [2.503(3) Å] but longer than that in the previously reported bis(σ-B-H) diisopropylaminoborane ruthenium complex [1.980(3) Å].[8] Although the benzylic C–H bond lengths, C1–H11 and C1–H12, show no specific elongation upon coordination according to X-ray diffraction, the DFT values indicate a significant lengthening for C1–H11 (*1.158* Å) in **3** versus *1.101* Å in **1**. The Ru1···H11 [1.97(3) Å, *1.897 Å*] and Ru1···C1 [2.375(3) Å, *2.376 Å*] distances are significantly shorter than those reported in the neutron diffraction study of the complex [$RuCl_2${PPh_2(2,6-$Me_2C_6H_3$)}$_2$], which displays two δ C–H methyl agostic interactions [Ru···H 2.113(11)/2.137(12) Å and Ru···C 2.637(7)/2.668(6) Å].[9] In **3**, the Ru1···C1 distance remains longer than Ru–C single-bond lengths for alkyl derivatives, and is superior to the sum of the covalent radii (2.22 Å),[10] but is certainly indicative of a strong agostic interaction.[11] The quality of the calculations is further confirmed by the excellent agreement between selected experimental and computed NMR parameters (see Figure S15).

A natural bond orbital (NBO) analysis of the electronic structure of **3** yielded a Lewis structure similar to that obtained for the bis σ-borane complexes already studied by our groups.[8,12] The 12-electron *fac*-ML_3 "$RuH_2(PCy_3)$" fragment is further stabilized by a three-center-four-electron symmetric ω-bond between the lone pair on the phosphorus of the phosphinoborane ligand and the σ(Ru-P) bond with PCy_3. In addition, donation from σ(B-H) and σ(C-H) into the respective σ*(Ru-H) in the *trans* position allows it to be an 18-electron configuration, formally. Natural localized molecular orbital (NLMO) composition of the coordinated σ-bonds indicated that donation from σ(B-H) is stronger than donation from σ(C-H) (see Table S1). The three nonbonding d orbitals on the "$RuH_2(PCy_3)$" fragment can participate in back-donation processes with various accepting orbitals. One such metal-centered lone pair, [LP_1(Ru)], has the proper

symmetry to interact both with σ*(B-H) and σ*(C-H), while another, [LP_2(Ru)], is suited to interact with the formally empty p atomic orbital on boron [LP*(B)]. The back-donation pattern is similar to what has been observed in bis(σ-borane) complexes.[8,12,13] The NBO analysis also revealed a donation from the σ(B-C) bond, thus explaining the slightly longer value observed for B–C in **3** with respect to **1**.

To obtain further insight into the properties of this new {η^2-C-H, η^2-B-H} fragment, we performed preliminary reactivity studies and found three different activation pathways upon exposure of **3** to H_2 and boranes. Pressurization of a C_6D_6 solution of **3** under 3 bar H_2 leads to B–C bond cleavage of the ligand, and quantitative and irreversible formation of **4** (Scheme 2).This reactivity contrasts with the hemilabile character of the phosphinoborane ligand observed

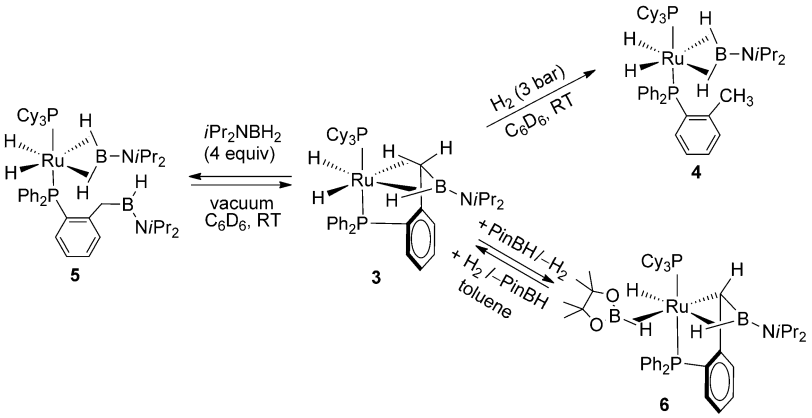

Scheme 2. Reaction of the bis(agostic) ruthenium complex **3** with dihydrogen, diisopropylaminoborane, and pinacolborane, thereby leading to **4**, **5**, and **6**, respectively.

for the complex **A** under the same reaction conditions.[2a] Reaction of **3** (C_6D_6, RT) with a fourfold excess of diisopropylaminoborane led to partial conversion into a new complex, **5**, in a 3:7 (**3**/**5**) phosphorus integration ratio. The complex **5** was clearly identified as the bis(σ-borane) ruthenium complex [RuH_2(η^2:η^2-H_2BN*i*Pr){$Ph_2PC_6H_4CH_2BH$(N*i*Pr_2)}(PCy_3)], thus resulting from the displacement of the two agostic bonds and coordination of diisopropylaminoborane at ruthenium. Drying the resulting mixture of **3** and **5** under vacuum restored **3**, with diisopropylaminoborane being stripped out (Scheme 2), thus illustrating the hemilability of the bis(agostic) fragment. Finally, reaction of **3** with pinacolborane led to the five-membered metallocycle complex **6** featuring a Ru–C single bond as a result of further activation of the agostic C–H bond in **3**, and loss of dihydrogen. Remarkably, the reaction is reversible as shown by exposure of **6** to dihydrogen, with the bis(agostic) complex **3** and free pinacolborane being restored, prior to transformation of **3** into **4**, because the presence of dihydrogen (Scheme 2).

The complex **6** was fully characterized by NMR spectroscopy and X-ray crystallography, and its formulation ascertained by DFT calculations (see computed geometry of **6** in the Supporting Information). At room temperature, the $^{31}P\{^1H\}$ NMR spectrum of **6** exhibits an AB pattern at $\delta =$ 53.76 and 57.44 ppm with a large coupling constant ($^2J_{PP} =$ 253 Hz) which is indicative of a *trans* disposition of the PCy_3 and the PPh_2 groups. The ^1H NMR spectrum at room temperature shows, in the hydride zone, three broad signals in a 1:1:1 integration ratio. The two BH signals at $\delta = -9.67$ (HBPin) and −5.92 ppm (HBN*i*Pr_2), and the terminal hydride at $\delta = -8.20$ ppm sharpen upon ^{11}B decoupling and ^{31}P decoupling, respectively.

Synthesis of the ^{13}C-enriched **6** ([^{13}C]-**6**) enabled the ^{13}C NMR assignment of the carbon atom directly bound to ruthenium ($\delta = 20.36$ ppm) with a large $^1J_{CH}$ coupling constant (140 ± 2 Hz), which is consistent with an uncoordinated C–H bond.

The X-ray structure of **6**, determined at 110 K (see Figure 2, Figure S16, and Tables S2 and S3), showed the presence, in the asymmetric unit, of two independent molecules (**6a** and **6b**) which present similar geometrical parameters.

The B2···Ru distance [2.171(5) Å (**6a**), 2.160(5) Å (**6b**), 2.163 Å (calcd)], the angle between the middle of [O,O], B2, and Ru [173.24°(**6a**), 171.46°(**6b**), 171.97°(calcd)], the elongated B2–H2 bond [1.33(5) Å(**6a**), 1.47(5)(**6b**), 1.39(calcd)], and the B2···H3 distance [2.16(5)(**6a**), 2.08(5)(**6b**), 2.218-(calcd)] are clearly in favor of a σ-B–H coordination mode of pinacolborane without any interaction between the terminal hydride H3 and the borane.[14] The Ru–C1 distance [2.184(4) Å (**6a**), 2.182(4) Å(**6b**), 2.173-(calcd)] is much shorter than in **3** [2.375(3) Å] and is within the range for Ru–C single-bond lengths.[11]

In summary, we have shown that the fourteen-electron fragment "RuH_2P_2" can be stabilized by two agostic δ C–H and ε B_{sp2}–H bonds. The resulting complex, [RuH_2({η^2-HB:η^2-HC-H-B-(N*i*Pr_2)$CH_2C_6H_4PPh_2$}(PCy_3)] (**3**), features a planar borane

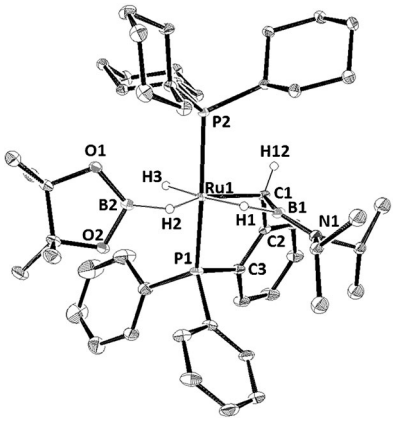

Figure 2. X-ray structure of **6**. Only **6a** is presented for clarity. Ellipsoids are shown at 30% probability. Hydrogen atoms of Cy, Ph, and *i*Pr groups as well as disordered *i*Pr groups have been omitted to avoid any ambiguity.

with two adjacent agostic interactions of different polarity. Hemilability of these two agostic bonds is demonstrated by coordination of diisopropylaminoborane and formation of the bis(σ-borane) ruthenium complex **5**. The integrity of the starting P–BHR ligand is preserved and the reaction is reversible under vacuum. In contrast, reaction of dihydrogen with **3** results in irreversible B–C bond cleavage and formation of the complex **4**. A third behavior is clearly demonstrated by reaction of **3** with pinacolborane: complete activation of the agostic C–H bond is achieved with the formation of the alkyl ruthenium complex **6**. Our findings show that C–H and B–H bond activation can be competitive within the same complex through the establishment of agostic bonds, a phenomenon directly relevant to the more general problem of selectivity in catalysis.

Experimental Section

o-$Ph_2PC_6H_4CH_2BH(NiPr_2)$ (**1**): An ethereal solution (20 mL) of *o*-$Ph_2PC_6H_4CH_2Li$·TMEDA (2.11 g, 5.29 mmol) was added to $ClHBNiPr_2$ (0.927 g, 6.29 mmol) in diethyl ether (5 mL) at −60 °C. The reaction mixture was stirred for 45 min at this temperature followed by 3 h at room temperature. The resulting dark-red solution was evaporated to dryness and toluene (20 mL) was added. After filtration over celite, removal of the solvent, pentane was added and the resulting suspension cooled to −50 °C and filtered. **1** was isolated as an off-white solid in 42% yield. Selected NMR data (C_6D_6, 298 K): $^{31}P\{^1H\}$ NMR (161.98 MHz): $\delta = -13.74$ ppm. $^{11}B\{^1H\}$ NMR (128.38 MHz): $\delta = 41$ ppm (br). ^1H NMR (400.13 MHz): $\delta = 0.89$ and 1.09 (d, $^3J_{HH} = 6.4$ Hz, 2×6H, CH_3 *i*Pr), 2.76 (dd, $^4J_{PH} = 2.4$ Hz, $^3J_{CHBH} = 2.8$ Hz, 2H, CH_2B), 3.00 and 3.73 (hept, $^3J_{HH} = 6.4$ Hz, 2×1H, CH *i*Pr), 4.92 (br, 1H, BH), 6.90–7.50 ppm (m, 14H, CH arom.). $^{13}C\{^1H\}$ NMR (100.61 MHz): $\delta = 21.9$ and 26.7 (s, 2×2C, CH_3 *i*Pr), 27.1 (br, CH_2B), 45.3 and 49.0 ppm (s, 2×1C, CH *i*Pr). Elemental analysis (%) calcd for $C_{25}H_{31}BNP$: C 77.53; H 8.07; N 3.62; found: C 77.62; H 8.14; N 3.54.

$[RuH_2\{\eta^2\text{-HB}:\eta^2\text{-HC-HB}(NiPr_2)CH_2C_6H_4PPh_2\}(PCy_3)]$ (**3**): A toluene solution (2 mL) of **1** (0.217 g, 0.559 mmol) was added to a toluene suspension (3 mL) of **2** (0.373 g, 0.558 mmol) and stirred at room temperature for 1 min. After removal of the solvent, pentane (5 mL) was added, and the suspension stirred 1 min before evaporation to dryness. This step was repeated until a golden powder was obtained. Then, cold pentane (6 mL) was added, the suspension was cooled to −55 °C and filtered. A yellow powder was separated and dried under vacuum leading to pure **3** in 70% yield. Crystals were grown at −38 °C from a saturated pentane solution. Selected NMR data: $^{31}P\{^1H\}$ NMR (C_6D_6, 298 K, 161.98 MHz): $\delta = 68.66$ (d, $^2J_{PP} = 241.4$ Hz, PPh_2), 72.10 ppm (d, $^2J_{PP} = 241.4$ Hz, PCy_3). $^{11}B\{^1H\}$ NMR (C_7D_8, 298 K, 128.38 MHz): $\delta = 35.5$ ppm (br). ^1H (C_7D_8, 183 K, 500.33 MHz): $\delta = -13.22$ (br, 1H, RuH), −8.58 (br, 1H, RuH), −6.71 (br, 1H, BH), −1.00 ppm (br, 1H, BCH···Ru), T_{1min} (C_7D_8, 500.33 MHz): $\delta = -11.2$ (273 K, 220 ms, RuH_2), −6.41 (273 K, 217 ms, BH), −0.96 ppm (263 K, 207 ms, BCH···Ru). $^{13}C\{^1H\}$ NMR (C_6D_6, 298 K, 100.61 MHz): $\delta = -11.24$ (br, BCH_2), 21.93, 22.03, 24.20 and 26.26 (s, CH_3 *i*Pr), 46.20 and 53.86 ppm (br, CH *i*Pr). Elemental analysis (%) calcd for $C_{43}H_{66}BNP_2Ru$: C 67.00; H 8.63; N 1.82; found: C 67.29; H 8.58; N 1.71.

$[RuH_2(\eta^2\text{:}\eta^2\text{-}H_2BNiPr)(Ph_2PC_6H_4CH_3)(PCy_3)]$ (**4**): At room temperature, an NMR tube containing a C_6D_6 solution of **3** (10.4 mg, 0.014 mmol) was pressurized with dihydrogen (3 bar) for 17 h. Selected NMR data for **4** (C_6D_6, 298 K): $^{31}P\{^1H\}$ NMR (161.98 MHz): $\delta = 57.35$ (d, $^2J_{PP} = 227.0$ Hz, PPh_2Tol), 78.01 ppm (d, $^2J_{PP} = 227.0$ Hz, PCy_3), $^{11}B\{^1H\}$ NMR (128.38 MHz): $\delta = 46.0$ ppm (br) ^1H NMR (400.13 MHz): $\delta = -11.58$ (dd, 2H, $^2J_{HP1} = 24.8$ Hz, $^2J_{HP2} = 23.2$ Hz, RuH_2), −6.29 (br, 2H, RuH_2B), 2.79 ppm (s, 3H, $C_6H_4CH_3$).

$[RuH_2(\eta^2\text{:}\eta^2\text{-}H_2BNiPr)\{Ph_2PC_6H_4CH_2BH(NiPr_2)\}(PCy_3)]$ (**5**): iPr_2NBH_2 (11.7 mg, 0.104 mmol) was added to a C_6D_6 solution of **3** (20.0 mg, 0.026 mmol) in a J. Young valve NMR tube. Selected NMR data for **5** (C_6D_6, 298 K): $^{31}P\{^1H\}$ NMR (161.98 MHz): $\delta = 55.37$ (d, $^2J_{PP} = 228.0$ Hz, PPh_2), 78.97 ppm (d, $^2J_{PP} = 228.0$ Hz, PCy_3). $^{11}B\{^1H\}$ NMR (128.38 MHz): $\delta = 46.0$ ppm (br). ^1H NMR (400.13 MHz): $\delta = -11.64$ (ψt, 2H, $^2J_{HP1} = {}^2J_{HP2} = 25.0$ Hz, RuH_2), −6.24 (br, 2H, RuH_2B), 3.38 (br, 2H, CH_2B), 5.00 ppm (br, 1H, CBHN).

$[RuH(\eta^2\text{-HB}:\kappa\text{C-HB}(NiPr_2)CHC_6H_4PPh_2)(\eta^2\text{-HBPin})(PCy_3)]$ (**6**): At room temperature, pinacolborane (1.2 equiv, 35 μL, 0.241 mmol) was added to a toluene solution of **3** (155.7 mg, 0.202 mmol) and the resulting solution was stirred for 1 h, until it became orange. After removal of the volatiles under vacuum, pentane (5 mL) was added and the solution cooled to −35 °C. **6** precipitated as a white solid. It was separated by filtration and dried under vacuum (141.0 mg, 78%). Selected NMR data for **6** (C_7D_8, 273 K): $^{31}P\{^1H\}$ NMR (202.55 MHz): $\delta = 53.76$ (d, $^2J_{PP} = 253$ Hz, PCy_3), 57.44 ppm (d, $^2J_{PP} = 253$ Hz, PPh_2), ^1H NMR (500.330 MHz): $\delta = -9.67$ (br, 1H, Ru*H*BPin), −8.20 (br, 1H, Ru*H*), −5.92 (br, 1H, Ru*H*BN), 1.95 ppm (br, 1H, RuC*H*).

CCDC 972214 (**1**), 972213 (**3**), and 999500 (**6**) contain the supplementary crystallographic data for this paper. These data can be obtained free of charge from The Cambridge Crystallographic Data Centre via www.ccdc.cam.ac.uk/data_request/cif.

Received: April 28, 2014
Revised: May 12, 2014

Keywords: agostic interactions · boron · hydrides · ligand design · ruthenium

[1] a) *The Chemistry of Pincer Compounds* (Eds.: D. Morales-Morales, C. M. Jensen), Elsevier Science B.V., Amsterdam, **2007**, p. 450; b) *Organometallic Pincer Chemistry*, *Vol. 40* (Eds.: G. van Koten, D. Milstein), Springer, Berlin, **2013**, p. 356; c) C. Gunanathan, D. Milstein, *Acc. Chem. Res.* **2011**, *44*, 588–602.

[2] a) Y. Gloaguen, G. Alcaraz, A.-F. Pécharman, E. Clot, L. Vendier, S. Sabo-Etienne, *Angew. Chem.* **2009**, *121*, 3008–3012; *Angew. Chem. Int. Ed.* **2009**, *48*, 2964–2968; b) Y. Gloaguen, G. Alcaraz, A. S. Petit, E. Clot, Y. Coppel, L. Vendier, S. Sabo-Etienne, *J. Am. Chem. Soc.* **2011**, *133*, 17232–17238.

[3] a) M. Ogasawara, M. Saburi, *Organometallics* **1994**, *13*, 1911–1917; b) D. G. Gusev, M. Madott, F. M. Dolgushin, K. A. Lyssenko, M. Y. Antipin, *Organometallics* **2000**, *19*, 1734–1739.

[4] J. E. Barquera-Lozada, A. Obenhuber, C. Hauf, W. Scherer, *J. Phys. Chem. A* **2013**, *117*, 4304–4315.

[5] M. Brookhart, M. L. H. Green, G. Parkin, *Proc. Natl. Acad. Sci. USA* **2007**, *104*, 6908–6914.

[6] a) G. Alcaraz, S. Sabo-Etienne, *Coord. Chem. Rev.* **2008**, *252*, 2395–2409; b) G. Alcaraz, M. Grellier, S. Sabo-Etienne, *Acc. Chem. Res.* **2009**, *42*, 1640–1649.

[7] H. Braunschweig, R. D. Dewhurst, T. Herbst, K. Radacki, *Angew. Chem.* **2008**, *120*, 6067–6069; *Angew. Chem. Int. Ed.* **2008**, *47*, 5978–5980.

[8] G. Alcaraz, A. B. Chaplin, C. J. Stevens, E. Clot, L. Vendier, A. S. Weller, S. Sabo-Etienne, *Organometallics* **2010**, *29*, 5591–5595.

[9] a) W. Baratta, E. Herdtweck, P. Rigo, *Angew. Chem.* **1999**, *111*, 1733–1735; *Angew. Chem. Int. Ed.* **1999**, *38*, 1629–1631; b) W. Baratta, C. Mealli, E. Herdtweck, A. Ienco, S. A. Mason, P. Rigo, *J. Am. Chem. Soc.* **2004**, *126*, 5549–5562.

[10] B. Cordero, V. Gomez, A. E. Platero-Prats, M. Reves, J. Echeverria, E. Cremades, F. Barragan, S. Alvarez, *Dalton Trans.* **2008**, 2832–2838.

[11] a) S. Burling, E. Mas-Marzá, J. E. V. Valpuesta, M. F. Mahon, M. K. Whittlesey, *Organometallics* **2009**, *28*, 6676 – 6686; b) R. T. Baker, J. C. Calabrese, S. A. Westcott, T. B. Marder, *J. Am. Chem. Soc.* **1995**, *117*, 8777 – 8784; c) W. Baratta, P. Da Ros, A. Del Zotto, A. Sechi, E. Zangrando, P. Rigo, *Angew. Chem.* **2004**, *116*, 3668 – 3672; *Angew. Chem. Int. Ed.* **2004**, *43*, 3584 – 3588; d) W. Baratta, A. Del Zotto, G. Esposito, A. Sechi, M. Toniutti, E. Zangrando, P. Rigo, *Organometallics* **2004**, *23*, 6264 – 6272.

[12] G. Bénac-Lestrille, U. Helmstedt, L. Vendier, G. Alcaraz, E. Clot, S. Sabo-Etienne, *Inorg. Chem.* **2011**, *50*, 11039 – 11045.

[13] a) Y. Gloaguen, G. Bénac-Lestrille, L. Vendier, U. Helmstedt, E. Clot, G. Alcaraz, S. Sabo-Etienne, *Organometallics* **2013**, *32*, 4868 – 4877; b) G. Alcaraz, E. Clot, U. Helmstedt, L. Vendier, S. Sabo-Etienne, *J. Am. Chem. Soc.* **2007**, *129*, 8704 – 8705; c) G. Alcaraz, L. Vendier, E. Clot, S. Sabo-Etienne, *Angew. Chem.* **2010**, *122*, 930 – 932; *Angew. Chem. Int. Ed.* **2010**, *49*, 918 – 920.

[14] S. Lachaize, K. Essalah, V. Montiel-Palma, L. Vendier, B. Chaudret, J. C. Barthelat, S. Sabo-Etienne, *Organometallics* **2005**, *24*, 2935 – 2943.

